Swift Observation of long GRB 090422

T. N. Ukwatta (GSFC/GWU), C. B. Markwardt (GSFC/UMD), M. Perri (ASDC), G. Stratta (ASDC), A. A. Breeveld (MSSL/UCL), S. D. Barthelmy (GSFC), D. N. Burrows (PSU), P. Roming (PSU), N. Gehrels (GSFC), for the Swift Team

1 Introduction

BAT triggered on GRB 090422 at 03:35:16 UT (Trigger 349931) (Ukwatta, *et al.*, *GCN Circ.* 9185). This was a 0.064 sec rate-trigger on a long burst with $T90 = 8.5 \pm 0.4$ sec. Swift slewed immediately to the burst. Narrow field instruments started observations at $\sim T + 64$ sec, and our best position is the UVOT-enhanced XRT location RA($J2000$) = 294.74967 deg (19h38m59.92s), Dec($J2000$) = +40.38445 deg (+40d23′04.0″) with an uncertainty of 1.5 arcsec (90% confidence, including boresight uncertainties), reported by Beardmore *et al.*, *GCN Circ.* 9194.

This burst has also been observed by Fermi GBM as reported by McBreen *et al.*, *GCN Circ.* 9228.

2 BAT Observation and Analysis

Using the data set from $T - 60$ to $T + 243$ sec, further analysis of BAT GRB 090422 has been performed by BAT team (Markwardt, *et al.*, *GCN Circ.* 9195). The BAT ground-calculated position is RA($J2000$) = 294.746 deg (19h38m59.1s), Dec($J2000$) = 40.398 deg (+40d23′52.1″) ± 2.0 arcmin, (radius, systematic and statistical, 90% containment). The partial coding was 72% (the bore sight angle was 21.4 deg).

The mask-weighted light curve (Fig. 1) shows two main peaks at $T + 0$ and $T + 8$ sec. They are each about 1 sec wide. There is a third, weaker peak at $\sim T = 50$ sec (see Fig. 2). $T90$ (15-350 keV) is 8.5 ± 0.4 sec (estimated error including systematics).

The time-averaged spectrum from $T - 0.4$ to $T + 8.5$ sec is best fit by a simple power-law model. The power law index of the time–averaged spectrum is 1.72 ± 0.30. The fluence in the $15 - 150$ keV band is $2.3 \pm 0.4 \times 10^{-7}$erg cm^{-2}. The 1-sec peak photon flux measured from $T - 0.37$ sec in the $15 - 150$ keV band is 1.7 ± 0.2 ph/cm2/sec. All the quoted errors are at the 90% confidence level.

The results of the batgrbproduct analysis are available at http://gcn.gsfc.nasa.gov/notices_s/349931/BA/

3 XRT Observations and Analysis

The XRT team has analyzed the complete data set of Swift-XRT data obtained from GRB 090422, starting from $T + 70$ s and ending at $T + 504$ ks.

The best position of the X-ray afterglow is the UVOT-enhanced XRT position (Beardmore , *et al.*, *GCN Circ.* 9194) is

RA(J2000) = 19h 38m 59.92s
Dec(J2000)= +40d 23' 04.0"

with an uncertainty of 1.5 arcsec (radius, 90% confidence).

The 0.3–10 keV X-ray light curve (Fig. 5) is well described by a double broken power-law model with decay indices $\alpha_1 = 2.1 \pm 0.2$, $\alpha_2 = 0.4 \pm 0.3$, $\alpha_3 = 1.1 \pm 0.1$ and temporal breaks $t_1 = 354 \pm 92$ s and $t_2 = 2.4 \pm 0.5$ ks.

The average X-ray spectrum from $T + 85$ s to $T + 70$ ks is well fitted by an absorbed power-law model with a photon index of 2.5 ± 0.2 and a column density of $(2.3 \pm 0.7) \times 10^{21}$cm^{-2} in excess

to the Galactic one in the direction of the source (1.7×10^{21}cm^{-2}, Kalberla *et al.*, 2005). The count-rate to observed (unabsorbed) 0.3–10 keV flux conversion factor deduced from this spectrum is $3.6\,(8.7)^{-11}$erg cm^{-2} count^{-1}.

The results of the XRT-team automatic analysis are available at
http://www.swift.ac.uk/xrt_products/00349931.

4 UVOT Observation and Analysis

The Swift/UVOT observed the field of GRB 090422 starting 55 s after the BAT trigger. Settled exposures started at $T + 74$ s with a Finding Chart (FC) in the white filter. No afterglow is detected at the enhanced position of the XRT afterglow (Beardmore, *et al.*, *GCN Circ.* 9194) nor at the position of the candidate found by the Liverpool Telescope (Guidorzi, *et al.*, *GCN Circ.* 9197). 3–sigma upper limits for detecting a source in the white and u FCs, and subsequent co-added images in all filters are:

Filter	Tstart (s)	Tstop (s)	Exposure (s)	Magnitude
white (FC)	74	224	147	>20.5
u (FC)	287	537	246	>19.6
v	617	11744	1317	>20.3
b	542	18318	1145	>20.8
u	690	24099	2059	>20.8
uvw1	666	23300	2203	>21.0
uvm2	641	22393	2092	>20.8
uvw2	592	10831	1318	>20.8
white	566	5591	341.4	>20.8

Table 1: Magnitude limits from UVOT observations

The quoted upper limits have not been corrected for the expected Galactic extinction along the line of sight corresponding to a reddening of $E_{B-V} = 0.198$ mag (Schlegel, *et al.*, 1998, ApJS, 500, 525). All photometry is on the UVOT photometry system described in Poole *et al.*(2008, MNRAS, 383, 627).

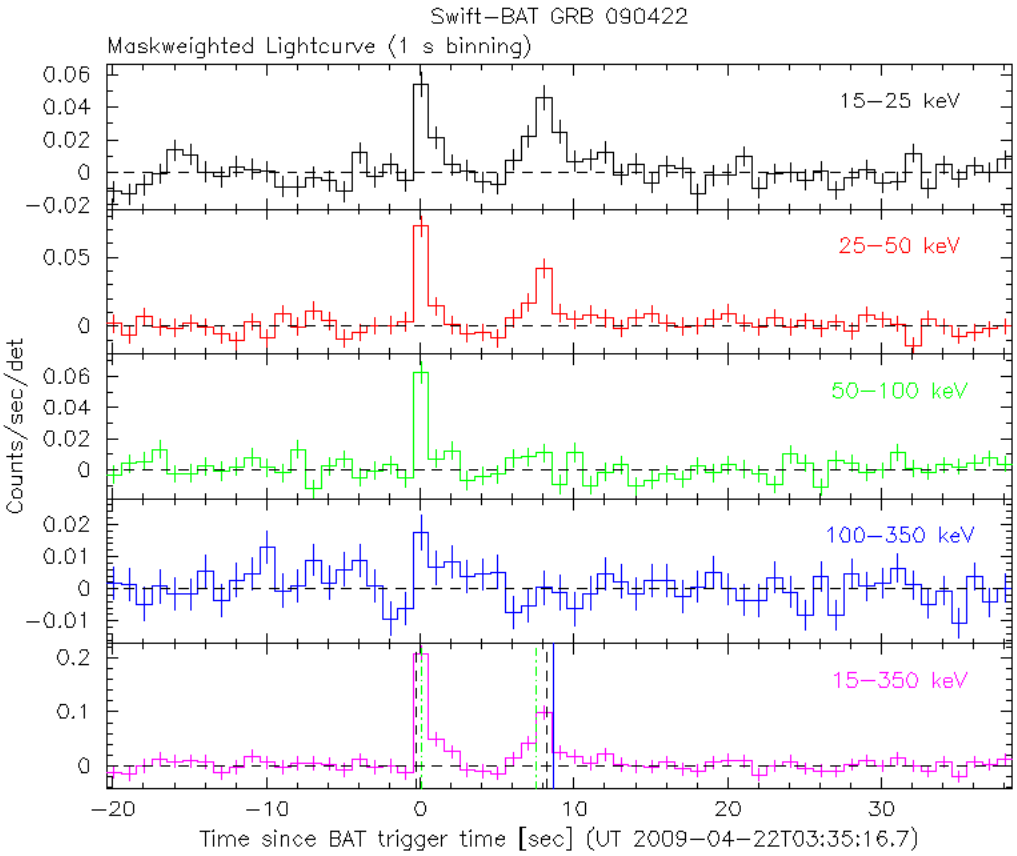

Figure 1: The mask-weighted light curve in the 4 individual plus total energy bands. The units are counts/sec/illuminated-detector and T_0 is 03:35:16 UT.

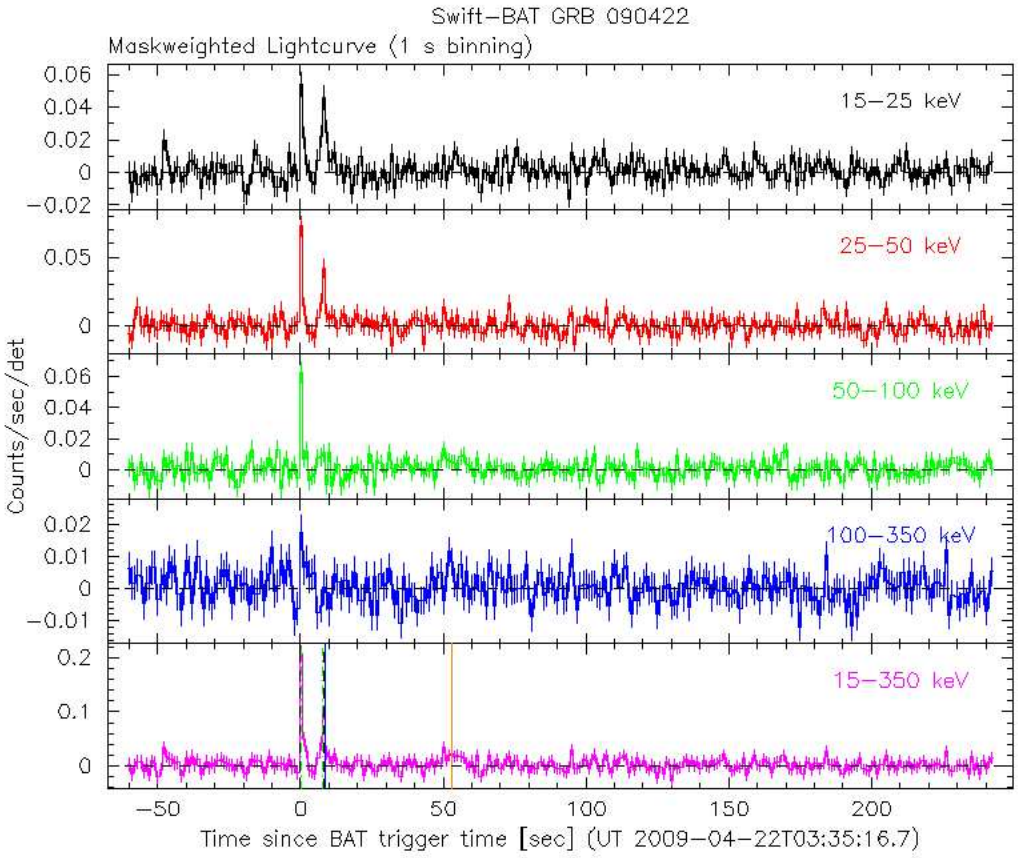

Figure 2: The mask-weighted light curve in the 4 individual plus total energy bands showing a weak peak around $T + 50$ seconds. The units are counts/sec/illuminated-detector and T_0 is 03:35:16 UT.

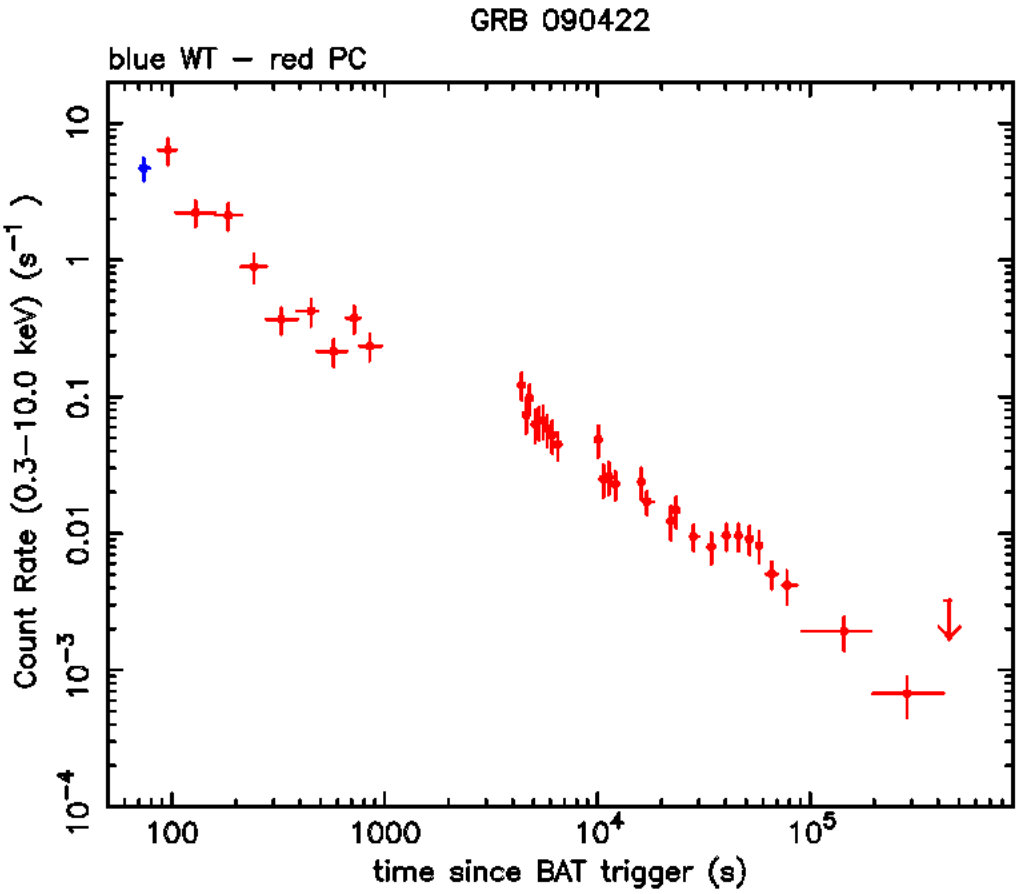

Figure 3: XRT Lightcurve. Counts/sec in the 0.3−10 keV band: Window Timing mode (blue), Photon Counting mode (red). The approximate conversion is 1 count/sec = $\sim 3.6 \times 10^{-11}$ ergs/cm^2/sec.

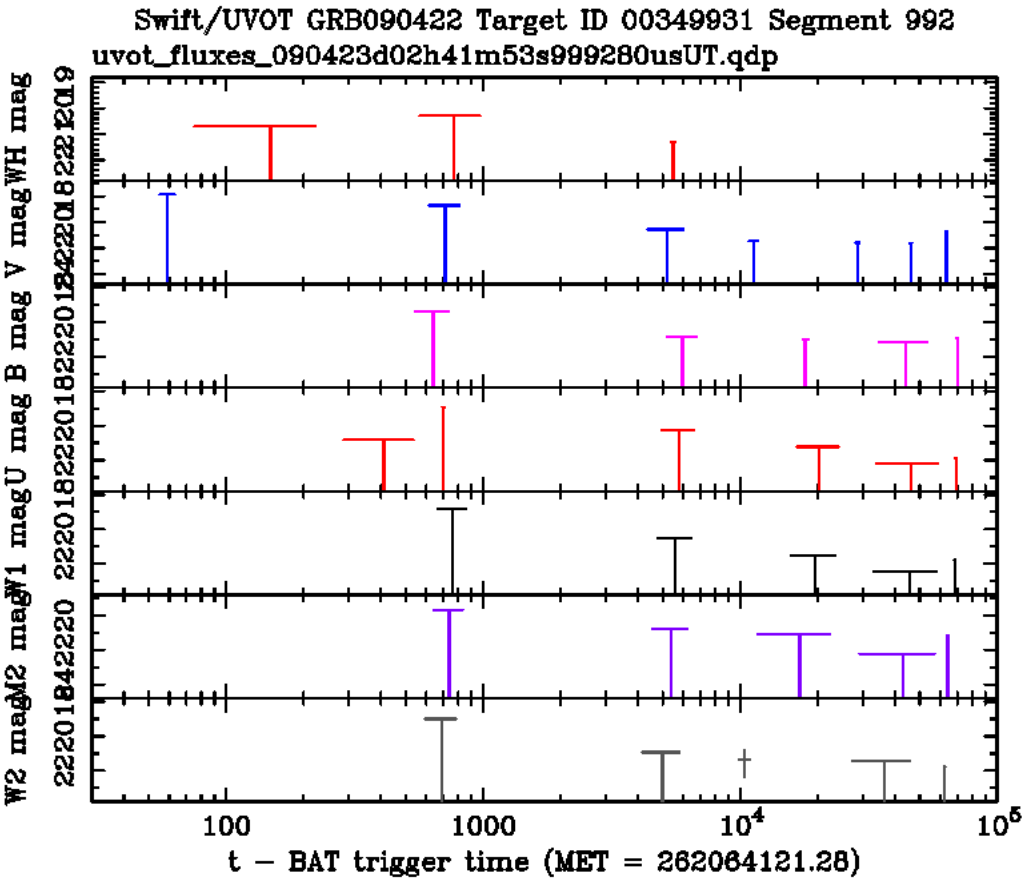

Figure 4: UVOT light curves.

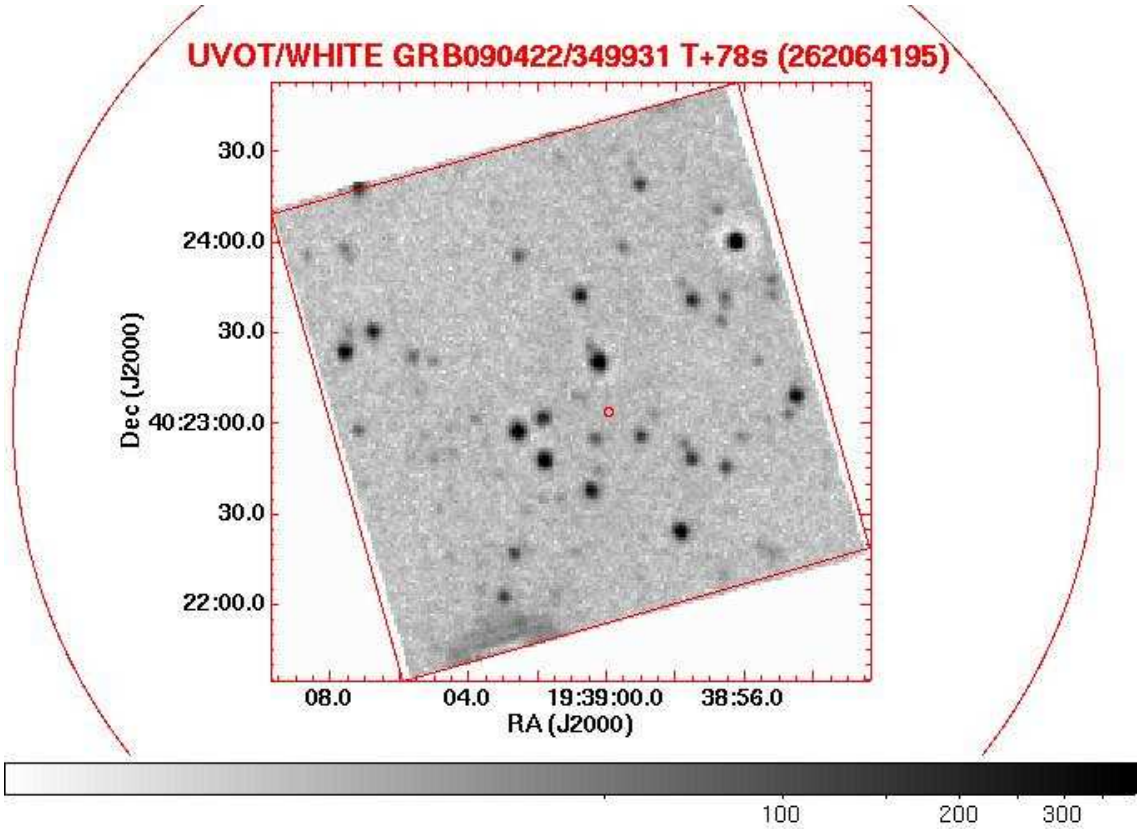

Figure 5: UVOT finding chart image. The large red circle is the BAT error region; a small red circle is the XRT error region. The UVOT position is indicated with a red box arbitrarily sized to 5 arc sec on a side.